Supplementary Material

A green metal-organic framework to monitor water contaminants

Priscilla Rocío-Bautista[a], Verónica Pino[a,*], Juan H. Ayala[a], Catalina Ruiz-Pérez[b], Oriol Vallcorbá[c]. Ana M. Afonso[a], Jorge Pasán[b,*]

[a]Departament of Chemistry, Analytical Chemistry Division, University of La Laguna, Tenerife, 38206 Spain
[b] Laboratorio de Rayos X y Materiales Moleculares (MATMOL), Physics Department, University of La Laguna, Tenerife, 38206 Spain
[c]ALBA Synchrotron, Cerdanyola del Valles, Barcelona, 28003, Spain.

Table of contents

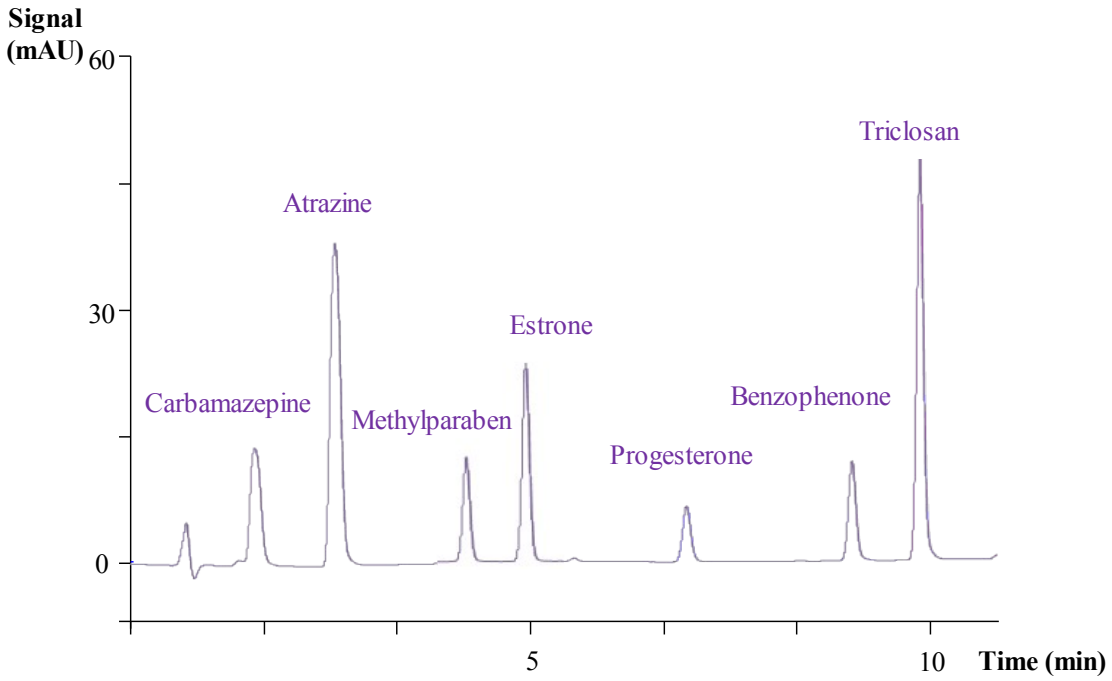

Figure S1. Representative chromatogram of the separation of seven target emerging pollutants. The concentration level of the standard is 100 $\mu g \cdot L^{-1}$ (in ACN). The UV-Vis detector was set at 220 nm. The UHPLC-UV-Vis separation required a binary mobile phase ACN:water at 0.4 $mL \cdot min^{-1}$ flow rate with the following gradient: initially 40% of ACN, increasing linearly this percentage up to 85% in 20 min. Remaining conditions as described in the experimental section.

s

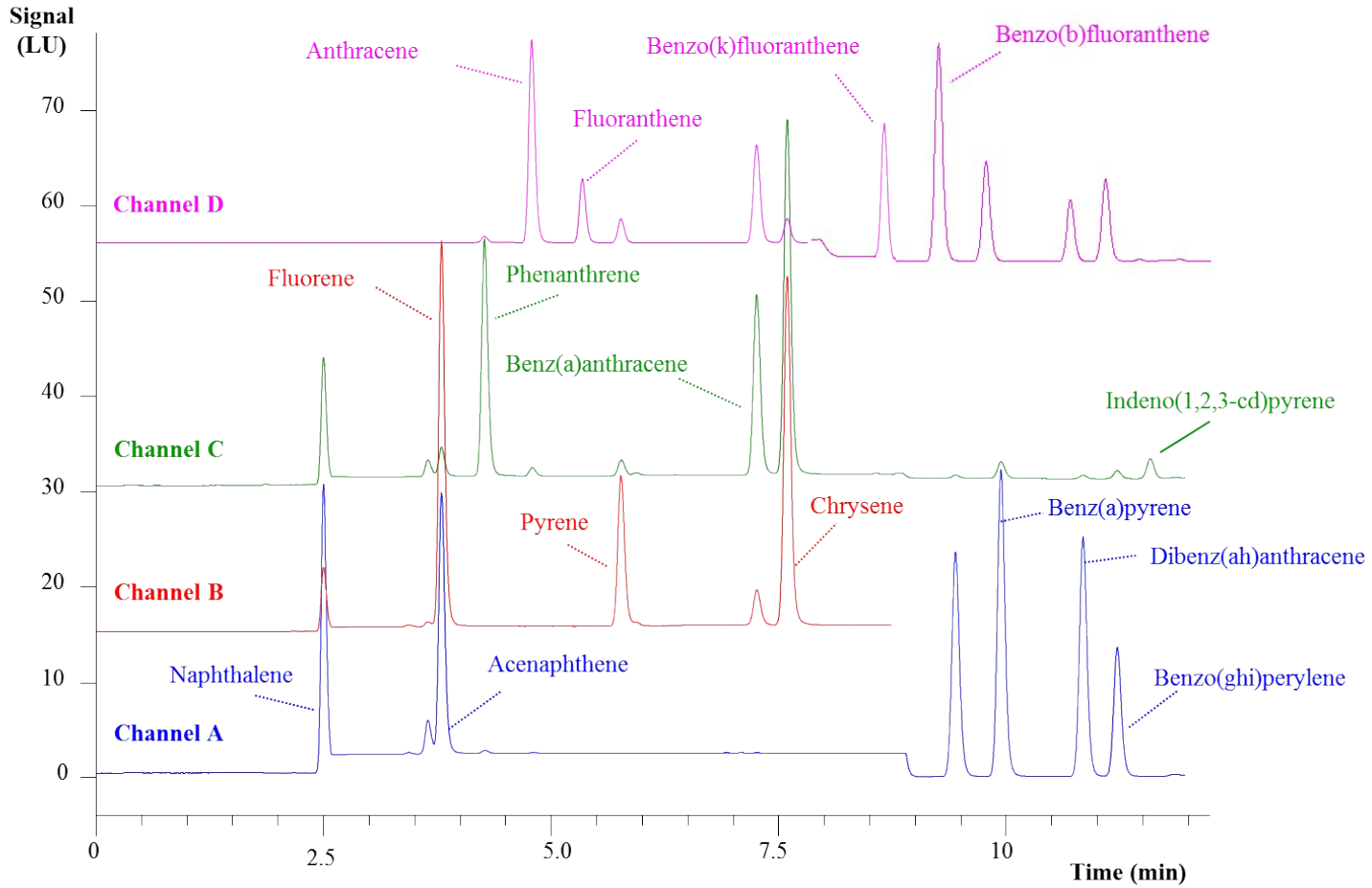

Figure S2. Representative chromatogram of the separation of PAHs by UHPLC-FD, with the wavelength program included in Table S2. The concentration level of the standard is 20 $\mu g \cdot L^{-1}$ (in ACN). The UHPLC-FD separation required a binary mobile phase ACN:water at 1 $mL \cdot min^{-1}$ flow rate: initially 50% of ACN, and increasing up to 100% of ACN in 11 min, keeping these conditions for 5 min.

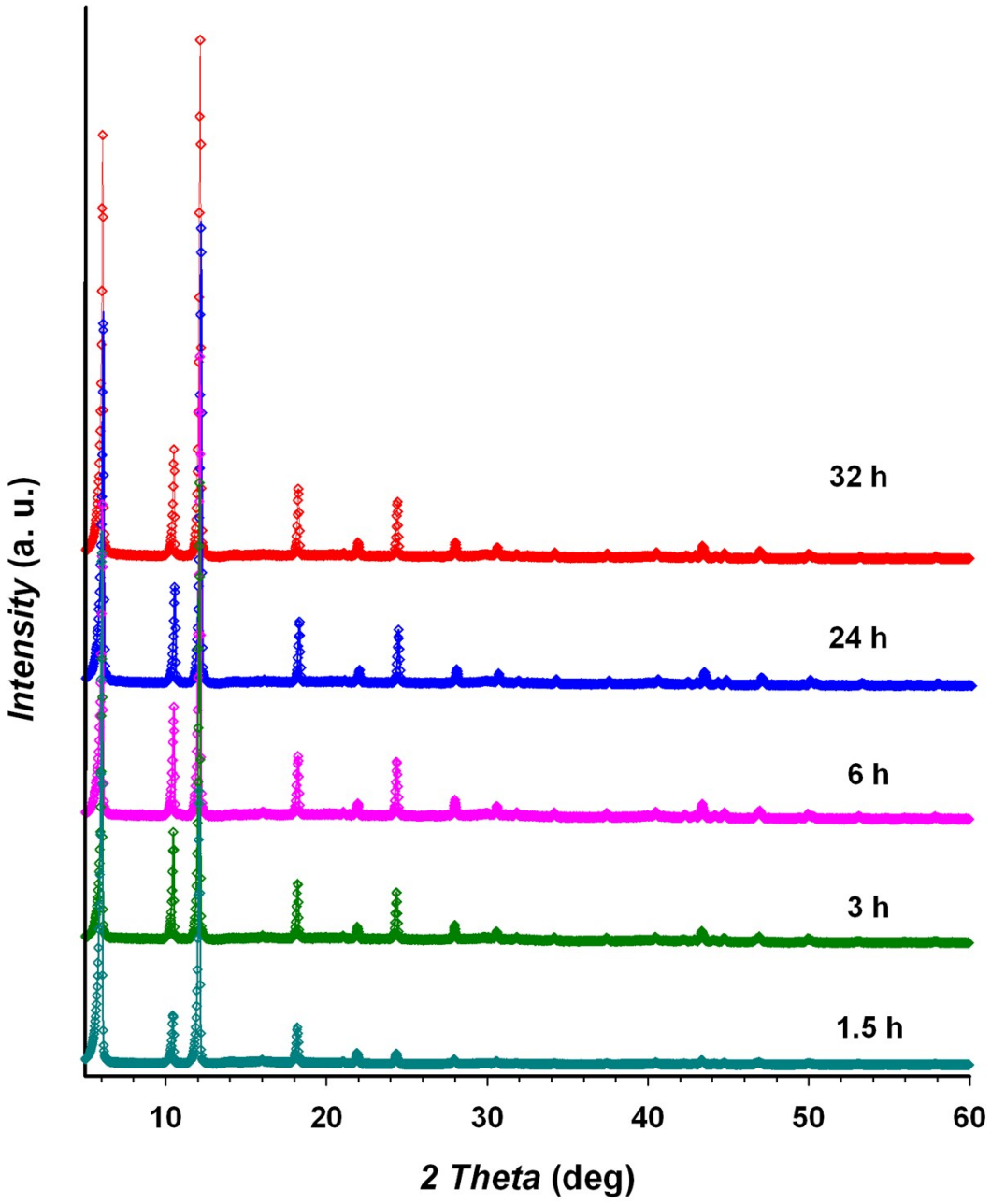

Figure S3. Powder X-ray diffraction patterns collected at the lab diffractometer (λ = 1.5418 Å) in the 5-80° angular range of the as synthetized products at different reaction times, following the procedure described in the Experimental Section.

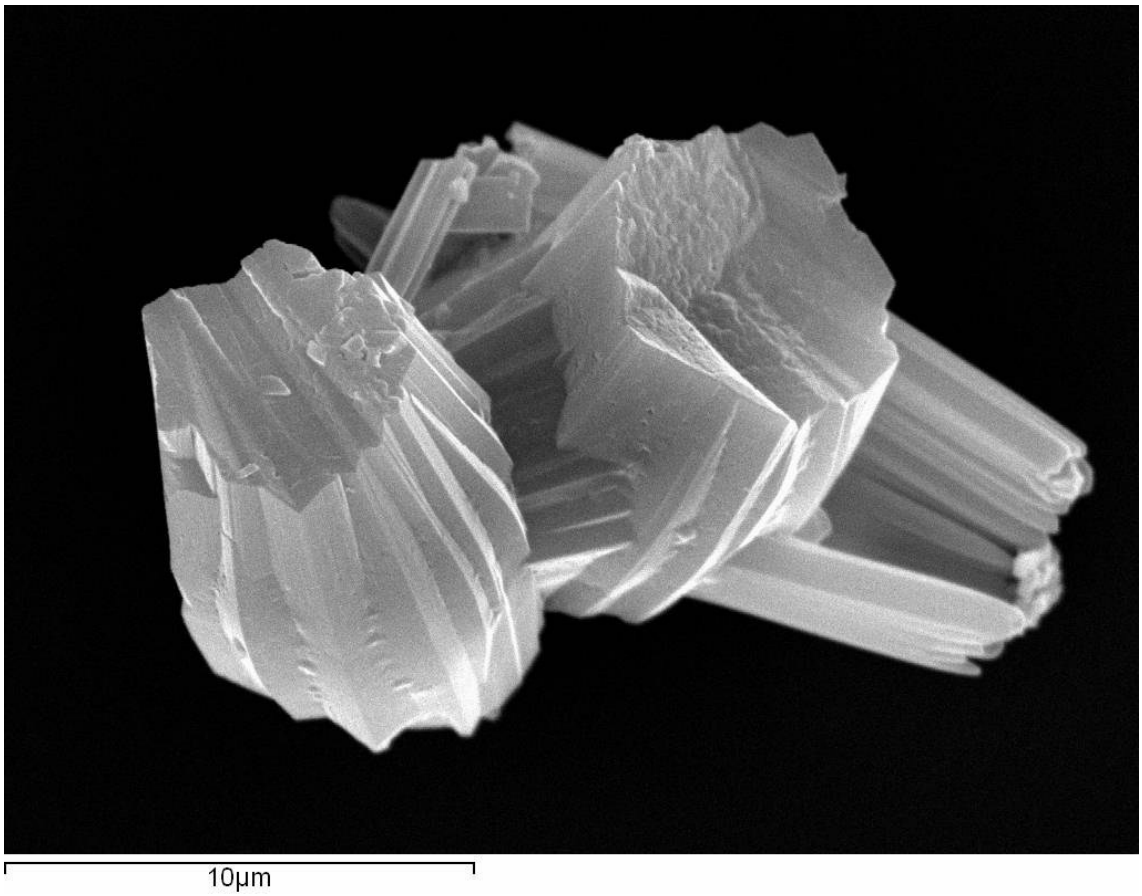

Figure S4. Scanning Electron Microscopy image of the CIM-80 crystallites.

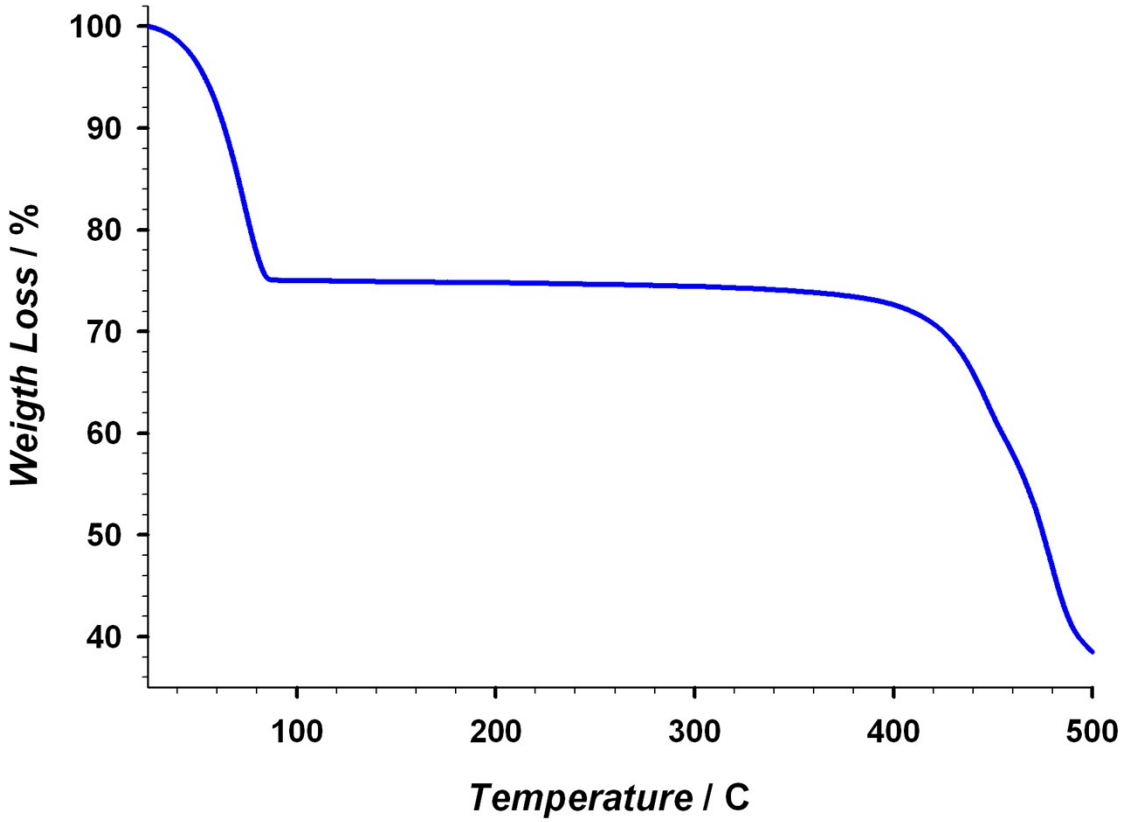

Figure S5. TG/DTA analysis of CIM-80.

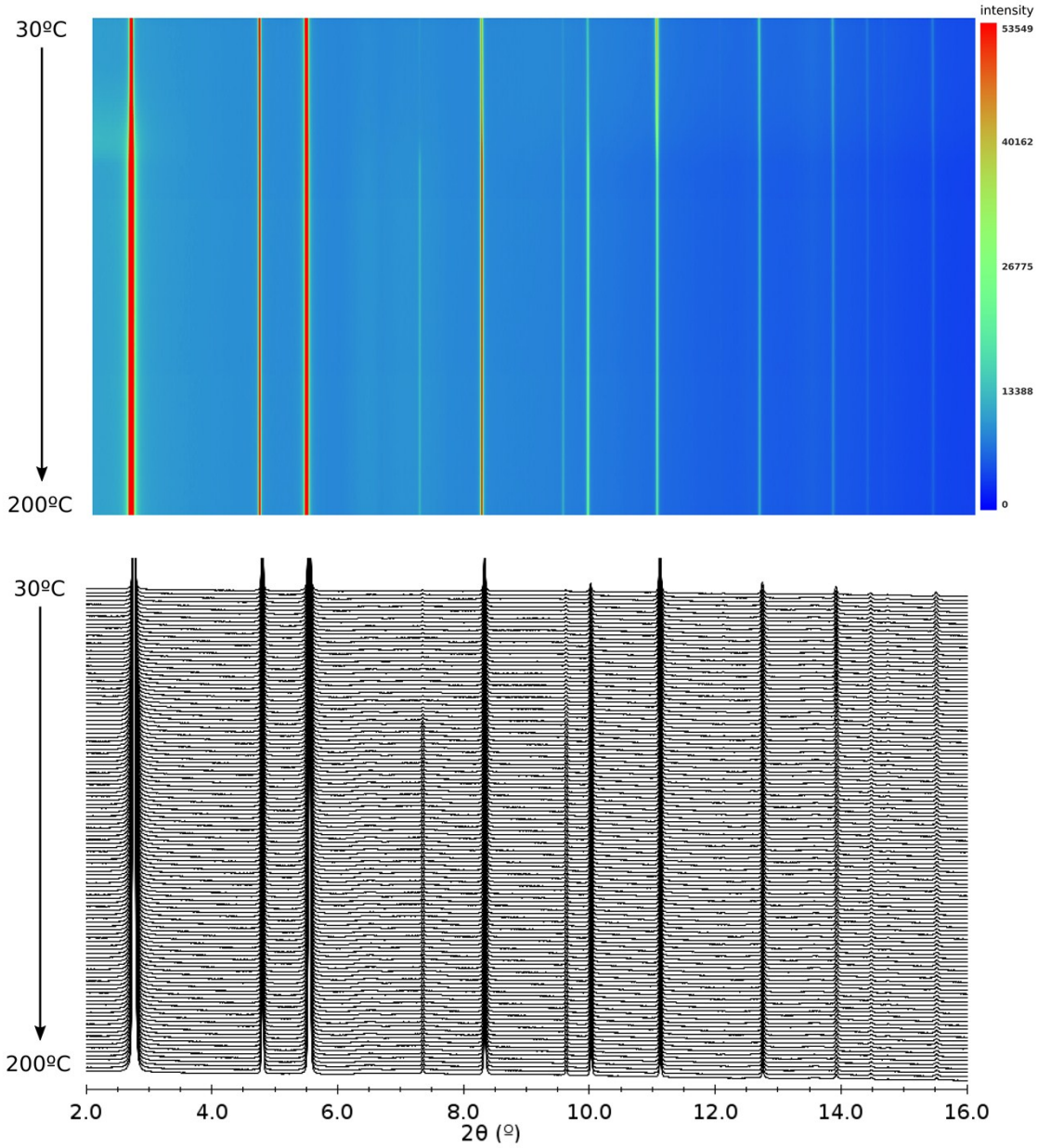

Figure S6. Thermodiffractogram of CIM-80 from 30 to 200 °C performed at BL04-MSPD beamline at ALBA synchrotron with λ = 0.70815.

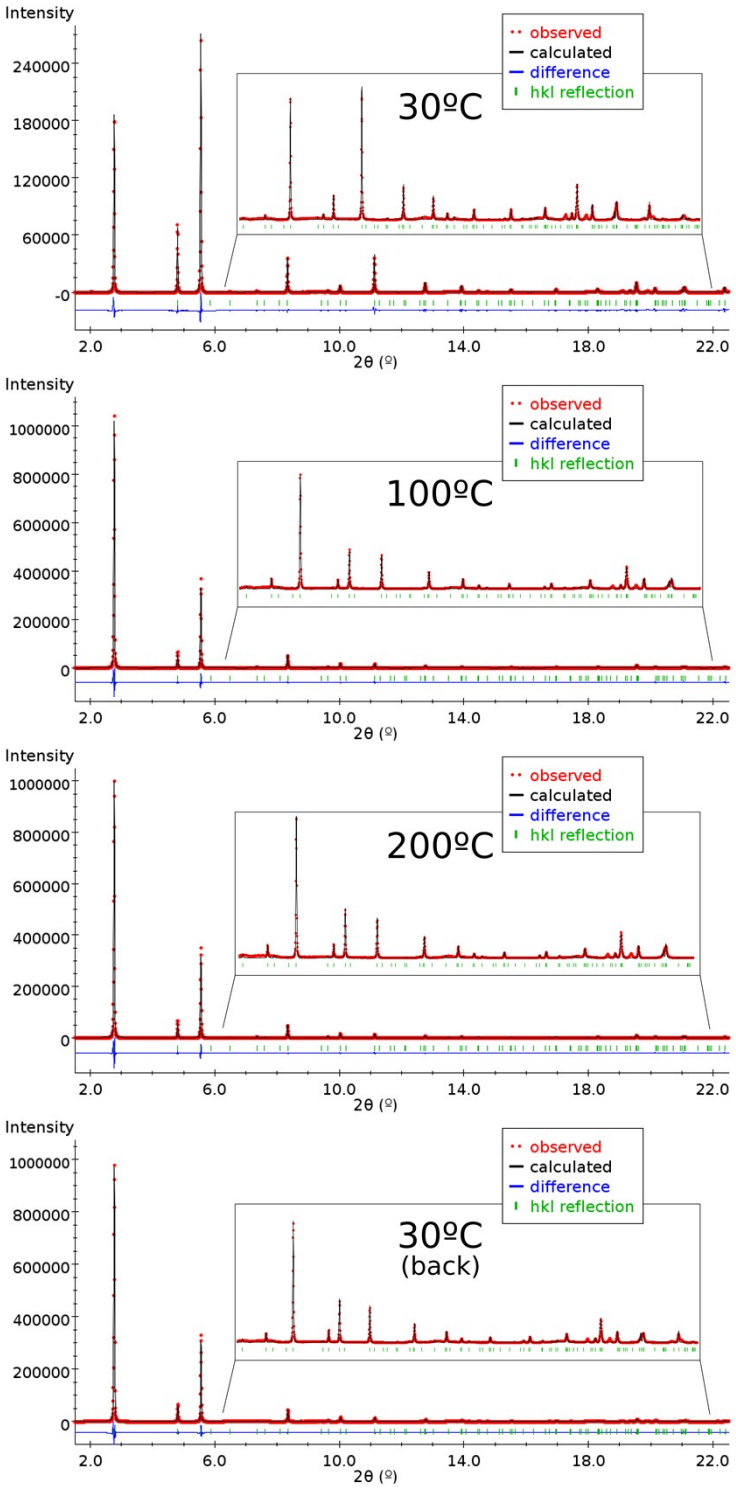

Figure S7. Profile matching of the powder diffraction patterns at selected temperatures.

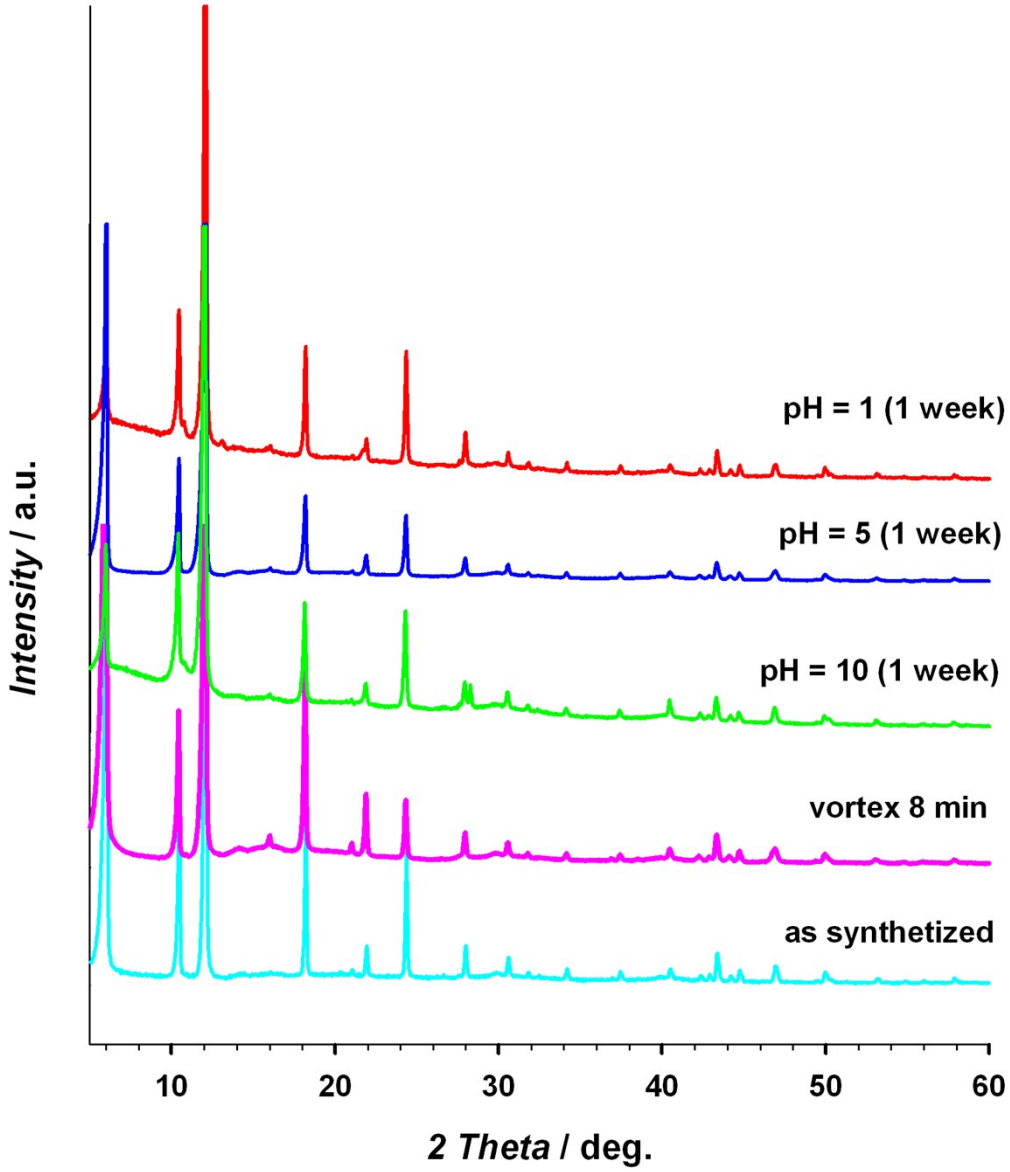

Figure S8. Diffraction patterns of CIM-80 after different stability tests, immersion in water at various pH values and application of vortex.

Figure S9. Images of the incubated cells in contact with the different tested concentrations of the MOF and the Alamar Blue reagent. Blue color indicates the lysis of the cells (none in this case), while pink color indicates the cells have not suffered any damage when they are put in contact with the MOF.

The cytotoxicity of the CIM-80 was evaluated using the Alamar Blue® cell viability assay as it was previously described [PLoS One. 2017;12:e0183795]. Briefly, the cell lines were put in contact with the MOF at different concentrations, ranging from 0.03 to 2 $mg \cdot mL^{-1}$, and incubated in 96-well plates for 24 h. Subsequently, the plates were analyzed by the microplate reader using a test wavelength of 570 nm and a reference wavelength of 630 nm. Dose response curves were plotted, and the 50% cytotoxic concentration (CC50) concentrations were calculated by linear regression analysis with 95% confidence limits. All experiments were performed two times each one, and the mean values were also calculated.

The Alamar Blue Assay Reagent® was provided by Biosource (Europe, Nivelles, Belgium) and the J774.1 murine macrophage cell line by ATCCTIB-67 (American Type Culture Collection LG Promochem, Spain).

A Tali® image cytometer (Thermo Fisher Scientific, Waltham, Massachusetts, USA) and an EnSpire® Multimode Plate Reader (Perkin Elmer, Madrid, Spain) were used.

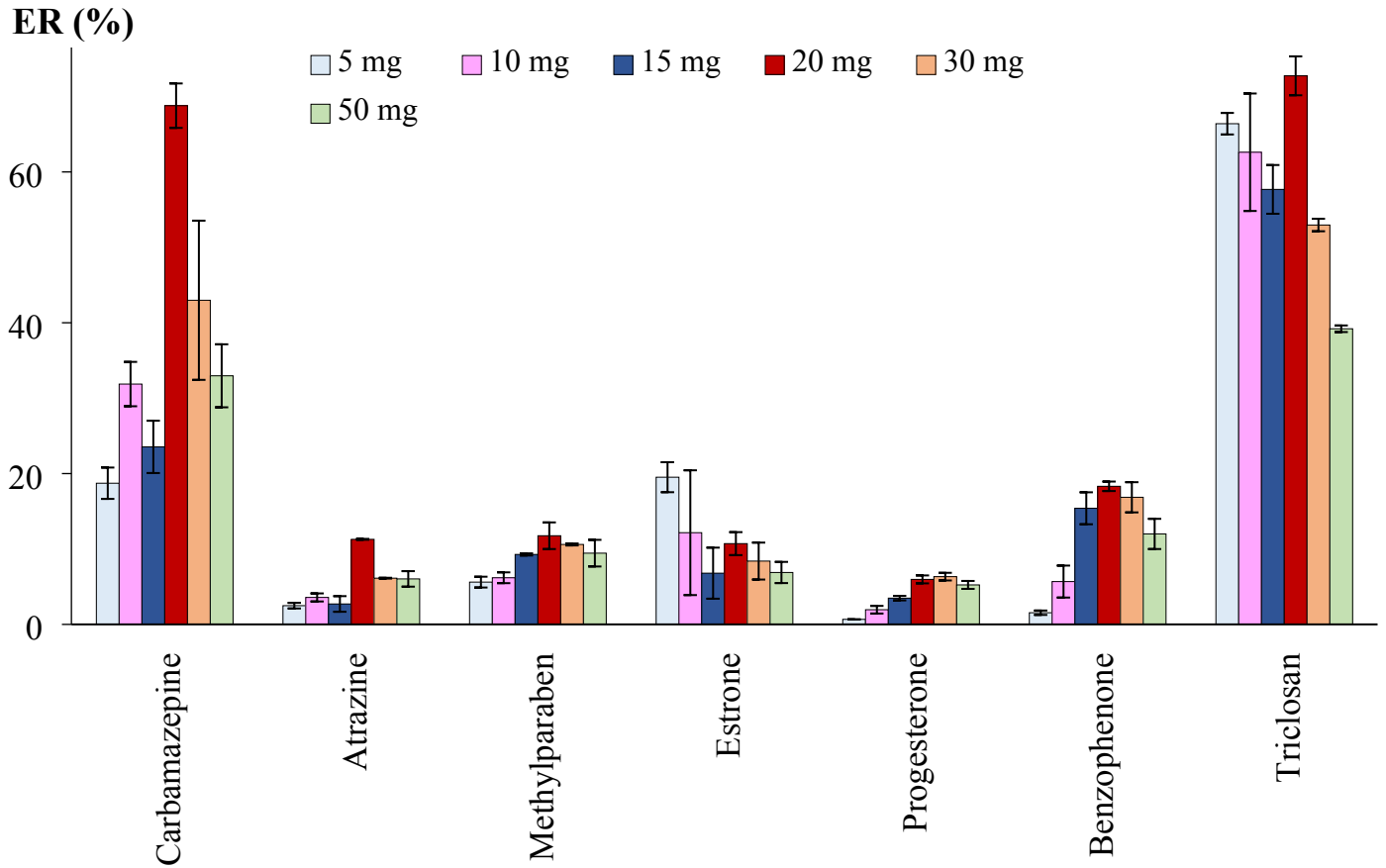

Figure S10. Influence of the amount of MOF CIM-80 in the entire extraction efficiency of the method for the group of emerging contaminants. Experiments were carried out by triplicate: 10 mL of water are mixed with 20 mg of CIM-80, then subjected to vortex stirring during 3 min. The supernatant aqueous phase is removed by centrifugation and decantation. Afterwards, 500 µL of ACN are added to the MOF remaining in the tube (and containing the trapped contaminants). Vortex is then applied for 3 min, followed again by centrifugation.

Table S1. Several characteristics of the group of analytes studied.

Analyte	Structure	Molecular weight ($g \cdot mol^{-1}$)	Volume[a] ($Å^3$)	Water solub.[a] ($mg \cdot L^{-1}$) at 25 ºC	$LogK_{OW}$[a]	pK_a[a]	Vapor press.[a] at 25 ºC (atm)
Carbamazepine	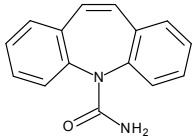	236.27	210.32	18	2.45	13.9	7.6×10^{-10}
Atrazine	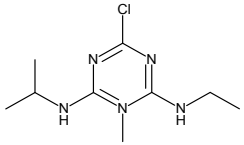	215.68	190.90	35 (26 °C)	2.61	2.27	1.7×10^{-8}
Methylparaben	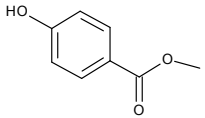	152.10	208.90	2.5×10^{-3}	1.96	8.50	3.15×10^{-7}
Estrone	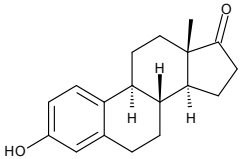	270.37	263.17	30	3.13	10.3	2.0×10^{-11}
Progesterone	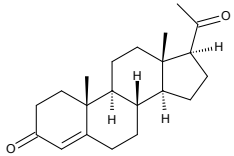	314.46	321.10	8.8	3.87	-	4.5×10^{-11}
Benzophenone	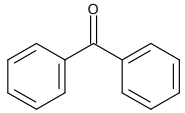	182.20	278.10	137	3.18	11.3	2.5×10^{-6}

Triclosan	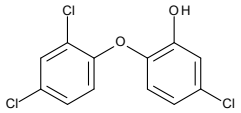	289.54	212.05	10 (20 ˚C)	4.76	7.80	4.3×10^{-8}
Naphthalene	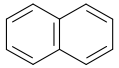	128.17	205.10	31	3.30	-	$1.0\cdot10^{-4}$
Acenaphthene	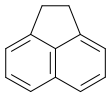	152.20	212.90	3.9	4.07	-	$1.2\cdot10^{-6}$
Fluorene	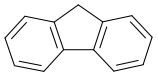	166.22	243.30	1.7	4.18	-	$7.9\cdot10^{-7}$
Phenanthrene	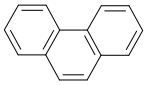	178.23	261.90	1.1	4.46	-	$1.6\cdot10^{-7}$
Anthracene	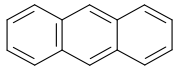	178.23	261.90	0.040	4.45	-	$1.0\cdot10^{-4}$
Fluoranthene	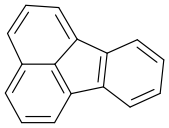	202.26	269.00	0.23	5.16	-	$1.2\cdot10^{-8}$
Pyrene	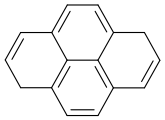	202.26	269.00	0.14	4.88	-	$5.\cdot10^{-10}$
Benz(a)anthracene	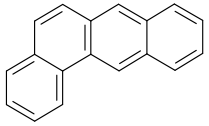	228.29	318.50	9.1×10^{-3}	5.79	-	$2.78\cdot10^{-7}$

Chrysene	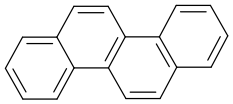	228.29	318.50	2.0×10^{-3}	5.73	-	$8.2\cdot10^{-12}$
Benzo(b)fluoranthene	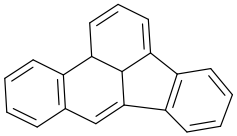	252.32	325.60	1.5×10^{-3}	6.60	-	$6.6\cdot10^{-10}$
Benz(a)pyrene	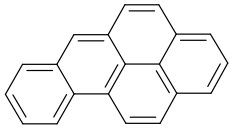	252.32	325.60	1.6×10^{-3}	6.13	-	$7.2\cdot10^{-12}$
Dibenz(a,h)anthracene	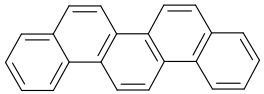	278.35	375.10	2.5×10^{-3}	6.50	-	$1.35\cdot10^{-12}$
Benzo(ghi)perilene	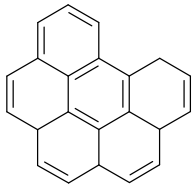	276.34	332.70	2.6×10^{-4}	6.63	-	$1.\cdot10^{-13}$
Benzo(k)fluoranthene	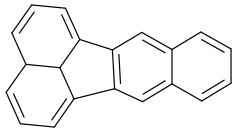	252.32	-	8.0×10^{-4}	6.11	-	$1.23\cdot10^{-12}$
Indeno(1,2,3-cd)pyrene	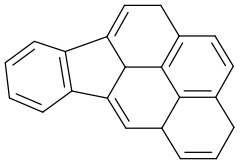	276.34	-	1.9×10^{-4}	6.70	-	$1.6\cdot10^{-13}$

[a]Obtained from SciFinder® 2018 database

Table S2. Wavelength program used in the FD for the UHPLC-FD determination of PAHs, indicating the four emission channels: A, B, C and D.

PAH	$\lambda_{ex\ max}$[a] (nm)	$\lambda_{em\ max}$[a] (nm)	time[b] (min)	λ_{ex} (nm)	λ_{em} (nm) in A	λ_{em} (nm) in B	λ_{em} (nm) in C	λ_{em} (nm) in D
			0	254	330	312	360	443
			2.0	214	330	312	360	443
Naphthalene	219	321	*2.5*[c]	214	330	312	360	443
			2.6	254	330	312	360	443
Acenaphthene	225	335	*3.6*[c]	254	330	312	360	443
Fluorene	262	311	*3.8*[c]	254	330	312	360	443
Phenanthrene	250	363	*4.3*[c]	254	330	312	360	443
Anthracene	250	424	*4.8*[c]	254	330	312	360	443
			5.2	280	330	312	360	443
			5.3	280	330	375	360	443
Fluoranthene	286	455	*5.4*[c]	280	330	375	360	443
Pyrene	273	371	*5.8*[c]	280	330	375	360	443
			6.9	280	330	375	385	443
			7.0	270	330	375	385	443
Benz(a)anthracene	286	386	*7.4*[c]	270	330	375	385	443
Chrysene	266	385	*7.7*[c]	270	330	375	385	443
			8.6	275	330	375	385	443
			8.7	275	406	375	385	443
			8.8	275	406	375	385	451
Benzo(b)fluoranthene	244	442	*9.0*[c]	275	406	375	385	451
Benzo(k)fluoranthene	290	410	*9.6*[c]	275	406	375	385	451
Benz(a)pyrene	284	405	*10.1*[c]	275	406	375	385	451
			10.5	275	406	375	496	451
			10.6	288	406	375	496	451
Dibenz(a,h)anthracene	295	404	*11*[c]	288	406	375	496	451
Benzo(ghi)perilene	272	470	*11.4*[c]	288	406	375	496	451
Indeno(1,2,3-cd)pyrene	276	307	*11.7*[c]	288	406	375	496	451

[a]maximum excitation and emission wavelength [Appl. Spectroscopy 51 (1998) 380] [b]only one wavelength can be modified at each time [c]average retention time

Table S3. Several quality analytical parameters of the UHPLC-UV method for 7 pollutants subjected study.

Analyte	Retention time ± SD[a]	Range (µg·L^{-1})	R	$S_{x/y}$[b]	Slope ± SD[c]	LOD[d] (µg·L^{-1})	LOQ[e] (µg·L^{-1})	RSD[f] (%)	
								Level 1[g]	Level 2[h]
Carbamazepine	1.6 ± 0.3	25 – 1000	0.9994	9331.4	910 ± 14	1.58	5.25	5.7	0.80
Atrazine	2.6 ± 0.1	25 – 1000	0.9998	10885	1491 ± 12	3.27	10.9	3.0	2.0
Methylparaben	4.1 ± 0.1	50 – 1000	0.9993	3194.1	797 ± 2	11.0	38.0	4.2	5.6
Estrone	4.8 ± 0.6	75 – 1500	0.9997	4035.2	272 ± 3	14.6	48.7	5.4	2.9
Progesterone	7.1 ± 0.5	50 – 1500	0.9998	9210.0	767 ± 6	11.9	39.7	3.6	2.1
Benzophenone	8.4 ± 0.5	25 – 1000	0.9999	2844.0	807 ± 5	2.21	7.40	6.8	4.9
Triclosan	9.9 ± 0.6	25 – 1250	0.9999	2683.8	569 ± 2	4.46	14.9	6.2	3.4

[a]standard deviation (n = 30, inter-day)
[b]standard deviation of the regression (or error of the estimate)
[c]confidence interval for the slope, associated to n = 6 calibration levels
[d]limit of detection
[e]limit of quantification
[f]relative standard deviation, as inter-day precision (n = 6, in 3 non-consecutive days)
[g]concentration level: 50 µg·L^{-1}
[h]concentration level: 800 µg·L^{-1}

Table S4. Several quality analytical parameters of the UHPLC-FD method for the PAHs studied.

Analyte	Retention time ± SD[a]	Range ($\mu g \cdot L^{-1}$)	R	$S_{x/y}$[b]	Slope ± SD[c]	LOD[d] ($\mu g \cdot L^{-1}$)	LOQ[e] ($\mu g \cdot L^{-1}$)	RSD[f] (%)	
								Level 1[g]	Level 2[h]
Naphthalene	2.5 ± 0.7	0.5 – 6	0.996	0.11	0.61 ± 0.03	0.03	0.1	4.1	3.6
Acenaphthene	3.6 ± 0.2	0.5 – 7	0.997	0.03	0.15 ± 0.01	0.06	0.2	4.5	2.5
Fluorene	3.8 ± 0.1	0.05 – 5	0.998	0.15	1.24 ± 0.03	0.006	0.02	4.9	1.4
Phenanthrene	4.32 ± 0.01	0.1 – 5	0.999	0.02	0.64 ± 0.01	0.03	0.09	3.1	2.0
Anthracene	4.8 ± 0.1	0.2 – 5	0.998	0.07	0.47 ± 0.02	0.015	0.05	8.0	4.0
Fluoranthene	5.40 ± 0.01	0.2 – 5	0.999	0.02	0.15 ± 0.01	0.015	0.05	3.4	1.8
Pyrene	5.86 ± 0.01	0.1 – 7	0.999	0.04	0.40 ± 0.01	0.009	0.03	5.6	4.8
Benz(a)anthracene	7.39 ± 0.01	0.1 – 5	0.994	0.11	0.46 ± 0.03	0.015	0.05	1.6	1.7
Chrysene	7.7 ± 0.2	0.05 – 4	0.999	0.06	0.85 ± 0.02	0.003	0.01	5.4	5.0
Benzo(b)fluoranthene	9.0 ± 0.1	0.1 – 5	0.997	0.05	0.30 ± 0.01	0.009	0.03	4.4	6.5
Benz(a)pyrene	9.6 ± 0.1	0.05 – 5	0.997	0.08	0.54 ± 0.02	0.003	0.01	6.2	5.9
Dibenz(a,h)anthracene	10.12 ± 0.01	0.05 – 5	0.995	0.21	0.63 ± 0.05	0.003	0.01	4.8	3.3
Benzo(ghi)perilene	11.0 ± 0.1	0.05 – 5	0.994	0.40	7.25 ± 0.51	0.006	0.02	6.2	10.9
Benzo(k)fluoranthene	11.4 ± 0.1	0.10 – 5.5	0.998	0.04	0.27 ± 0.01	0.006	0.02	6.5	5.4
Indeno(1,2,3-cd)pyrene	11.7 ± 0.1	0.5 – 8	0.999	0.01	0.08 ± 0.01	0.09	0.3	2.5	5.1

[a]standard deviation (n = 30, inter-day)
[b]standard deviation of the regression (or error of the estimate)
[c]confidence interval for the slope, associated to n = 7 calibration levels
[d]limit of detection
[e]limit of quantification
[f]relative standard deviation, as inter-day precision (n = 6, in 3 non-consecutive days)
[g]concentration level: 0.8 $\mu g \cdot L^{-1}$
[h]concentration level: 2 $\mu g \cdot L^{-1}$

Table S5. Analytical performance of methods reported in the scientific literature for the determination of similar water contaminants using SPE.

Contaminant	Sorbent (amount)	Sample prep.	LOD (ng·L^{-1})	Chromatographic method	Reference
Carbamazepine, estrone & triclosan	NVP[a] (2.5 mg)	BAμE[b]	5, 100 & 10	HPLC-DAD	Int. J. Environ. Anal. Chem. 97 (2017) 484
Atrazine	MWCNTs[d] (100 mg)	μSPE[c] cartidges	20	GC-MS	Sci. Total Environ. 396 (2008) 79
Estrone and derivatives	Oasis® HLB (-)	μSPE[c] disks	1.37	GC-MS	Sci. Total Environ. 590 (2017) 832
Progesterone	Poly(THF)[e] (-)	FPSE[f]	60	HPLC-MS/MS	J. Chromatogr. A 1437 (2016) 116
Carbamazepine, atrazine, progesterone, estrone & triclosan	MIL-53(Al) (5 mg)	D-μSPE[h]	13 – 21	HPLC-DAD	Talanta 179 (2018) 775 [19]
8 PAHs	Fe_3O_4/HKUST-1 (25 mg)	M-D-μSPE[i]	2.7 – 15	UHPLC-FD	J. Chromatogr. A 1436 (2016) 42 [10]
16 PAHs	CIM-80 20 mg)	D-μSPE[h]	0.75 – 9.3	UHPLC-FD	Present work
Carbamazepine, atrazine, progesterone, methylparaben, benzophenone, estrone & triclosan	CIM-80 (20 mg)	D-μSPE[h]	0.090 – 21 μg·L^{-1}	UHPLC-UV	Present work

[a]*N*-vinylpyrrolidone polymer
[b]bar-adsorptive microextraction
[c]miniaturized solid-phase extraction
[d]multiwalled carbon nanotubes
[e]sol–gel poly(tetrahydrofuran)
[f]fabric-phase sorptive extraction
[g]Quick, Easy, Cheap, Effective, Rugged, and Safe dispersive extraction method
[h]dispersive miniaturized solid-phase extraction
[i]magnetic-based dispersive miniaturized solid-phase extraction